Shielding Considerations for Satellite Microelectronics

Wesley C. Fan, Clifton R. Drumm, Stanley B. Roeske, and Gary J. Scrivner
Radiation and Electromagnetic Analysis Department
Sandia National Laboratories
Albuquerque, New Mexico 87185

Abstract

Shielding for space microelectronics needs to provide an acceptable dose rate with minimum shield mass. The analysis presented here shows that the best approach is, in general, to use a graded-Z shield, with a high-Z layer sandwiched between two low-Z materials. A graded-Z shield is shown to reduce the electron dose rate by more than sixty percent over a single-material shield of the same areal density. For protons, the optimal shield would consist of a single, low-Z material layer. However, it is shown that a graded-Z shield is nearly as effective as a single-material shield, as long as a low-Z layer is located adjacent to the microelectronics. A specific shield design depends upon the details of the radiation environment, system model, design margins/levels, compatibility of shield materials, etc. Therefore, we present here general principles for designing effective shields and describe how the computer codes are used for this application.

I. INTRODUCTION

The natural space radiation environment consists of three major components, electrons and protons trapped in the earth's magnetic field (Van Allen belts), protons from solar flares, and very high energy (> 0.1 GeV) charged particles (galactic cosmic rays). Satellite microelectronics are subject to these radiation environments, and often must be radiation hardened to meet their performance requirements.

The use of commercial, unhardened parts for satellite missions has several advantages over the use of radiation-hardened parts: lower cost, wider selection, and state-of-the-art capability. However, the radiation hardness of commercial electronics parts is not well known and may vary from batch to batch. Part requirements, including design margins, are often introduced to bound the variability, and significant radiation shielding may be required to protect these parts. Due to severe weight restrictions, however, it is important to avoid over-shielding.

The objectives of this study are: 1) to identify several specific orbits where natural electrons and protons are expected to provide a large dose to shielded microelectronics, 2) to evaluate the relative contributions of the primary and secondary (bremsstrahlung) radiation, and 3) to compare and evaluate shielding materials and to establish some design guidelines. The computational tools required to design the shields are also described. The conclusions drawn here may apply to a certain extent to other radiation effects besides total dose to silicon-based microelectronics, but other radiation effects are outside the scope of this analysis.

Previous studies of optimal shield configurations, Rossi, et al.[1] and Barnea, et al.[2], were directed at tissue dose and are not directly applicable to the shielding of microelectronics. Rossi, et al. designed a multilayer shield of minimum mass to provide a specified dose rate to human tissue. Their analysis, however, was based on approximate electron and photon transport models, which have been significantly improved in recent years. Barnea, et al. designed a two-layer shield to minimize the human-tissue dose

0018-9499/96$05.00

rate for a given shield mass-thickness. Their conclusions are valid for the shielding of electrons but may not be optimal for proton shielding. Barnea's study was based on Monte Carlo analyses, which can be quite time consuming for performing optimization studies, where many different shield configurations must be analyzed.

II. SPACE RADIATION ENVIRONMENTS

The near-earth, trapped space radiation environment, which extends from a few hundred kilometers in altitude to about ten earth radii, can be simply described by two regions. The outer zone consists of mainly trapped electrons and the inner zone consists of the slowly varying high-energy protons accompanied by the trapped electrons. The intensity and energy distribution of electrons and protons vary greatly with orbit altitude and, to a lesser extent, with orbit inclination. The optimal shield design depends on both the intensity and the energy distribution of the radiation.

There are several computer programs for estimating the average values of the natural trapped electrons and protons. The results presented here are from the commercial program SPACE RADIATION[3] and are based on the AE8MAX[4] model of electrons at solar maximum and the AP8MIN[5] model of protons at solar minimum. Our purpose here is to identify several specific radiation environments that are fairly difficult to shield against and to determine characteristics of various radiation shield materials.

In order to compare the various electron and proton spectra, we considered the dose to a thin silicon detector shielded by aluminum, as a function of the altitude of the orbit for several aluminum shield thicknesses. Figure 1 shows the silicon dose from natural electrons for circular orbits of 0° inclination, for altitudes up to 60,000 km. The well-known double-humped electron distribution is clearly illustrated, with the location of the peaks a weak function of the shield thickness. The maximum microelectronics dose due to natural electrons occurs near 4,000 km and 20,000 km altitude. The change in the shape of the curves for different shield thicknesses is a result of the spectral variation with altitude. The curves for different orbit inclinations exhibit similar characteristics.

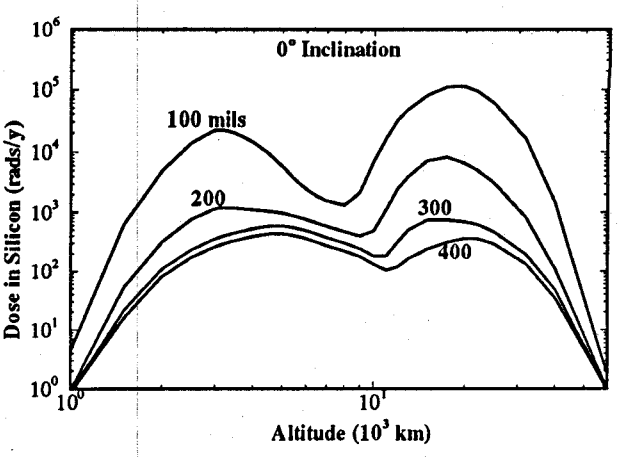

Fig. 1 Natural trapped electron dose in silicon versus altitude for slab aluminum shields of various thickesses.

Figure 2 shows the silicon dose from natural protons for altitudes up to 20,000 km, for 0°inclination. The maximum occurs at about 3,000 km altitude. For thicker shields, the maximum occurs at successively lower altitudes, where the proton spectra are harder.

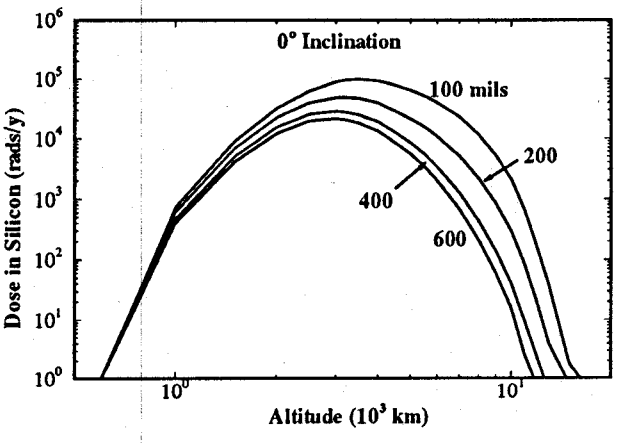

Fig. 2. Natural trapped proton dose in silicon versus altitude for slab aluminum shields of various thicknesses.

III. ELECTRON SHIELDING

Electron transport in matter is a complicated function of several distinct physical processes. Three of them are important for shielding space electrons: 1) inelastic scattering from atomic electrons, 2) elastic scattering from nuclei, and 3) the production of bremsstrahlung photons. Inelastic scattering of electrons results in energy loss without significant directional change. Inelastic scattering is characterized by a stopping power, which is the electron energy loss per unit path length. The electron stopping power (per unit areal density) is roughly proportional to the Z/A ratio, where Z is the atomic number and A is the atomic mass of the shield material. The Z/A ratio varies from 0.4 for tantalum, to 0.48 for aluminum, to nearly 1.0 for hydrogen. For this reason, low-Z materials are more effective for inelastic scattering of electrons. Physically, the reason for this is that the inelastic scattering is directly related to the density of atomic electrons in the shield material. High-Z nuclei have more neutrons than low-Z nuclei do. The additional neutrons add mass without increasing the shield effectiveness.

Electrons also undergo elastic scattering interactions with atomic nuclei, where electrons are deflected without significant energy loss. Elastic scattering interactions effectively reduce the electron penetration though the shield by deflecting electrons from the primary direction. Unlike inelastic scattering, the elastic scattering is roughly proportional to the Z^2/A ratio, so that high-Z materials are more effective for causing elastic scattering. A combination of low- and high-Z materials, by maximizing elastic and inelastic scattering effects, may provide the most effective shield for electrons.

The third physical process important in the shielding of electrons is the production of bremsstrahlung photons, which are emitted when electrons change direction or energy. Photons generally are harder to shield against than electrons, so the production of bremsstrahlung can significantly degrade shield effectiveness. Like elastic scattering, bremsstrahlung production is roughly proportional to the Z^2/A ratio, thus more photons are produced as electrons slow down in high-Z materials. On the other hand, high-Z materials are generally more effective in attenuating photons. This self-shielding effect somewhat mitigates the bremsstrahlung penalty of high-Z shields.

Because of the complicated interplay of the various processes involved in electron slowing down, it is not obvious which shield materials are the most effective for a given orbit. To make a quantitative assessment, we generated dose-vs-depth curves for the Global Positioning Satellite (GPS) natural electron environment (20,175-km altitude, 55° inclination, circular orbit, omnidirectional electrons). We used the CEPXS/ONELD[6] code package in these analyses.

Figure 3 compares the shielding effectiveness of low-Z (polypropylene and aluminum), mid-Z (kovar), and high-Z (tantalum) materials.

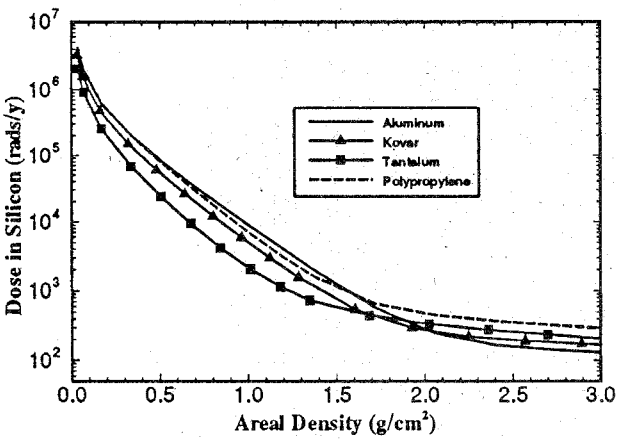

Fig. 3 Dose-vs-depth for omnidirectional natural trapped electrons at 20,175-km, 55°-inclination, circular orbit for single-material slab shields.

Up to an areal density of about 1.75 g/cm^2, where electron dose dominates, tantalum is the most effective shielding material. This region is apparently dominated by elastic scattering. Beyond 1.75 g/cm^2, however, tantalum is less effective and aluminum is a more effective shielding material. Contribution to absorbed dose in

this region is dominated by the bremsstrahlung *photons*, which is less for aluminum than for tantalum. Aluminum is a better shield than polypropylene, since, although bremsstrahlung photons are produced in aluminum, they are also attenuated more, resulting in a lower dose with the aluminum shield.

Based on these results and previous arguments, it seems feasible to design a layered shield to take advantage of the large elastic scattering cross section of high-Z materials and the low bremsstrahlung emission from low-Z materials. Figure 4 is a schematic diagram of a three-layer shield design. A low-Z material (aluminum) effectively shields the primary electrons due to its relatively large stopping power for electrons. This outer aluminum may be the satellite skin itself. Next is a layer of high-Z material (tantalum), which effectively scatters electrons and absorbs the secondary bremsstrahlung photons. Finally, a thin layer of low-Z material is located between the high-Z material and the microelectronics to suppress photo-electron emission.

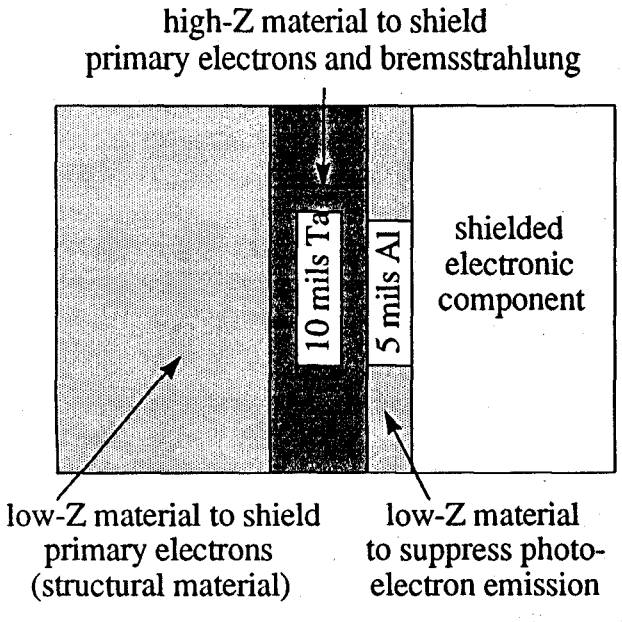

Fig. 4 Schematic of a three-layer shield design.

Figure 5 compares the shield effectiveness of a pure aluminum shield with an aluminum/tantalum/aluminum multi-layer shield. Silicon dose is shown for shields with combined areal density >1 g/cm^2. The layered shield includes a layer of aluminum, followed by 10 mils of tantalum and 5 mils of aluminum. These thicknesses were chosen for demonstration purposes, since the optimal values would depend on the details of a specific design. For the shielding thicknesses considered, the layered shield is at least sixty percent better than a pure aluminum shield. The benefits of the additional layer of tantalum are twofold. Tantalum provides further electron attenuation (the elastic scattering effect) in the region where electron dose dominates and further photon attenuation in the region where bremsstrahlung dose dominates. However, a thin layer of aluminum is necessary to reduce the secondary electron emission from tantalum. The multi-layer shield is able to take advantage of the large elastic scattering cross section of tantalum and the low bremsstrahlung emission from aluminum.

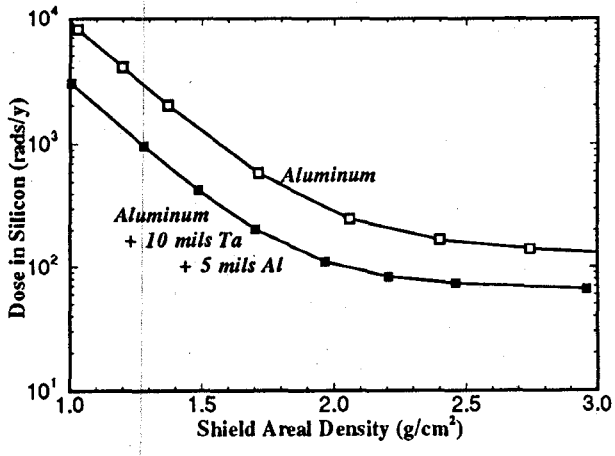

Fig. 5 Slab shield dose-vs-depth comparison for omnidirectional natural trapped electrons at 20,175-km, 55°-inclination, circular orbit.

IV. PROTON SHIELDING

A comparison of Figures 1 and 2 shows that the proton component of the natural environment may dominate the microelectronics dose for altitudes below about 9,000 km. Furthermore, protons are generally more difficult to shield than

are electrons. For this reason the proton environment must be considered when designing a shield for satellites designed to operate in the several-thousand km altitude range. Solar-flare protons are not specifically considered in this analysis, but the conclusions drawn here are also applicable to solar-flare protons.

Unlike electron transport, secondary particle production due to protons usually can be neglected. A notable exception to this is the neutron production from high-energy proton interactions, which is especially significant for high-Z targets. However, except for very thick high-Z shields (~5 g/cm^2 tantalum), the portion of the silicon dose from neutrons is less than 10% of the total and usually can be neglected[7].

With the neglect of secondary-particle production from proton interactions, proton shielding is more straightforward than electron shielding. Proton slowing down is dominated by inelastic scattering with atomic electrons. For this reason, the proton stopping power (per unit areal density) is roughly proportional to the Z/A ratio.

In this work we used the LITXS/ONELD code package[8] to model proton transport and slowing down. The LITXS code generates proton cross sections in the same format as the CEPXS code does for electrons and utilizes the same transport solver (ONELD), so that the modeling is quite efficient. The LITXS/ONELD code models one-dimensional geometries and has been extensively tested against other existing codes such as LAHET[9].

Figure 6 compares the silicon dose rate for several pure shield materials for a proton spectrum at 3,000 km altitude and 0° inclination. Although hydrogen is not a realistic candidate for a shielding material, it is included here for comparison purposes. Obviously, the lower-Z materials are more effective proton shields. A low-Z material such as polypropylene results in more than a factor of two greater dose reduction than does a high-Z material such as tantalum. Figure 7 shows the proton dose for the tantalum/aluminum shields compared with single-material shields. The thickness of the front layer is 0.5 g/cm^2 for both of the bilayer shields shown in Fig. 7.

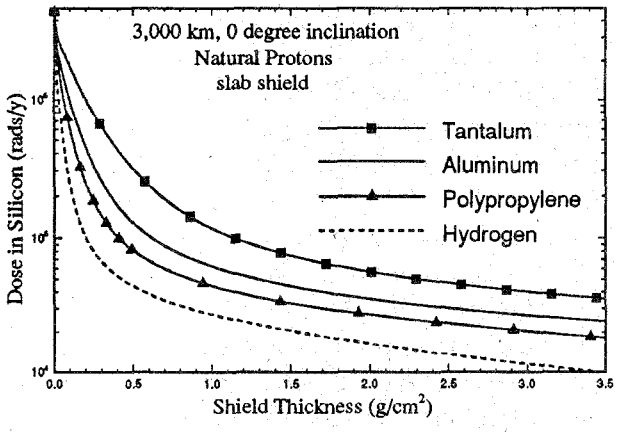

Fig. 6 Dose-vs-depth for natural trapped protons at 3,000 km, 0° inclination.

The significance of Figure 7 is that a shield with a high-Z layer may be nearly as effective as a pure aluminum shield, as long as there is a low-Z layer adjacent to the microelectronics. Therefore, the optimal electron shield, which consists of low-Z/high-Z/low-Z layers will be very effective for shielding protons as well, as long as the last low-Z layer is thick enough.

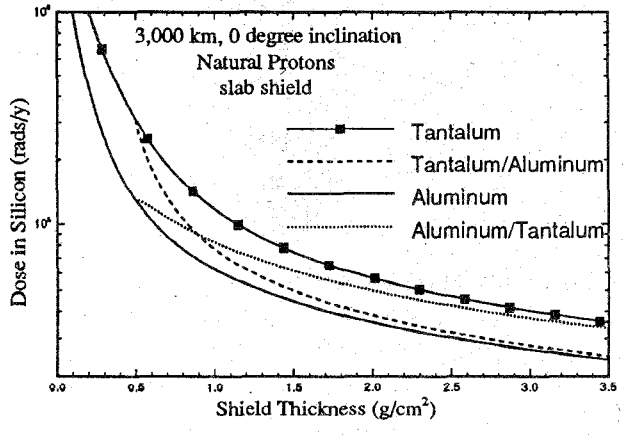

Fig. 7 Comparison of single-material and multi-layer shield effectiveness for natural trapped protons.

Figure 8 compares the effectiveness of a pure *aluminum* shield with the three-layer shield that is optimal for shielding electrons. The multi-layer shield is slightly less effective than the pure aluminum shield for shielding protons because of the presence of the tantalum layer. The effect of the tantalum is slight, however, since the tantalum layer is relatively thin.

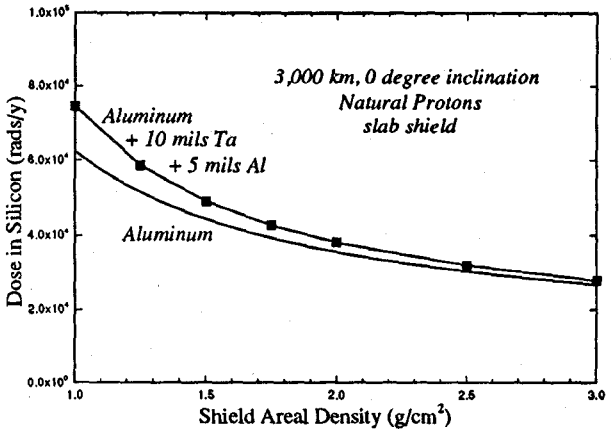

Fig. 8 Comparison of single-material and three-layer shield effectiveness for natural trapped protons.

V. SUMMARY

We have described a methodology for designing an optimal shield that consists of multiple layers of different shield materials. For electrons the optimal shield consists of a high-Z layer sandwiched between the two low-Z layers. For trapped electrons, a layered shield can result in more than a sixty percent reduction in dose over a single-material shield of the same areal density. In many applications the satellite structure and the part package already provide the outer and inner low-Z layers, so that the only addition required to the system is the high-Z material.

For protons, the optimal shield would consist of a single, low-Z material layer. However, it is shown that including a high-Z layer does not significantly degrade the proton-shielding effectiveness, as long as a low-Z layer is situated adjacent to the microelectronics. The present study has been limited to one-dimensional geometries, but the method can be extended to multidimensional shields by using the recently-developed code package CEPXS/TORT[10], which is a multidimensional extension of CEPXS/ONELD.

CEPXS/ONELD is readily available to the user community from the Radiation Shielding Information Center (RSIC) as code package CCC 544. At the present time, the LITXS code and the version of the CEPXS code that is used as a cross-section processor for TORT are research tools, not yet released to the community.

Acknowledgment

This work was supported by the U.S. Department of Energy under contract DE-AC04-94AL85000.

REFERENCES

[1] M. L. Rossi and M. C. Stauber, "Radiation Protection Design Considerations for Man in Geosynchronous Orbits," *IEEE Trans. Nucl. Sci.*, vol. NS-24, pp. 2248-2251, Dec. 1977.

[2] G. Barnea, M. J. Berger, and S. M. Seltzer, "Optimization Study of Electron-Bremsstrahlung shielding for Manned Spacecraft," *J. Spacecraft*, vol. 24, no.2, pp. 158-161, 1987.

[3] "SPACE RADIATION User's Manual," Severn Communications Corporation, 1990.

[4] J. I. Vette, "The AE-8 Trapped Electron Model Environment," NASA Goddard Space Flight Center, WDC-A-R&S 91-24, 1991.

[5] D. M. Sawyer and J. I. Vette, "AP-8 Trapped Proton Environment for Solar Maximum and Solar Minimum," National Space Science Data Center, NASA Goddard Space Flight Center, WDC-A-R&S 76-06, 1976.

[6] L. J. Lorence, Jr. "CEPXS/ONELD Version 2.0: A Discrete Ordinates Code Package for General One-Dimensional Coupled

Electron-Photon Transport," *IEEE Trans. Nucl. Sci.*, vol. 39, no. 4, pp. 1031-1034, Aug. 1992.

[7] C. R. Drumm, "Proton Transport Methods for Satellite Shield Modeling," SAND93-0200, Sandia National Laboratories Report, March 1993.

[8] C. R. Drumm, "Modeling of Spacecraft Proton Shielding by the Discrete Ordinates Method," *Trans. Am. Nucl. Soc.*, vol. 65, pp. 359-361, June 1992.

[9] R. E. Prael and H. Lichtenstein, "User Guide to LCS: the LAHET Code System," LA-UR-89-3014, Los Alamos National Laboratory, Los Alamos, New Mexico, 1989.

[10] C. R. Drumm, "Multidimensional Electron-Photon Transport with Standard Discrete Ordinates Codes," proceedings of the *American Nuclear Society Radiation Protection and Shielding Conference*, North Falmouth, MA, April 1996.